

Published in final edited form as:

J Immunol. 2009 January 1; 182(1): 216–224.

Progression of Pancreatic Adenocarcinoma Is Significantly Impeded with a Combination of Vaccine and COX-2 Inhibition¹

Pinku Mukherjee^{2,*}, Gargi D. Basu[†], Teresa L. Tinder^{*}, Durai B. Subramani^{*}, Judy M. Bradley^{*}, Million Arefayene[‡], Todd Skaar[‡], and Giovanni De Petris[§]

^{*}Department of Immunology, Mayo Clinic Arizona, Scottsdale, AZ 85259

[§]Department of Pathology, Mayo Clinic Arizona, Scottsdale, AZ 85259

[†]Translational Genomics Research Institute, Scottsdale, AZ 85259

[‡]Department of Medicine, Indiana University Cancer Center, Indianapolis, IN 46202

Abstract

With a 5-year survival rate of <5%, pancreatic cancer is one of the most rapidly fatal malignancies. Current protocols for the treatment of pancreas cancer are not as effective as we desire. In this study, we show that a novel Mucin-1 (MUC1)-based vaccine in combination with a cyclooxygenase-2 inhibitor (celecoxib), and low-dose chemotherapy (gemcitabine) was effective in preventing the progression of preneoplastic intraepithelial lesions to invasive pancreatic ductal adenocarcinomas. The study was conducted in an appropriate triple transgenic model of spontaneous pancreatic cancer induced by the KRAS^{G12D} mutation and that expresses human MUC1 as a self molecule. The combination treatment elicited robust antitumor cellular and humoral immune responses and was associated with increased apoptosis in the tumor. The mechanism for the increased immune response was attributed to the down-regulation of circulating prostaglandin E₂ and indoleamine 2, 3,-dioxygenase enzymatic activity, as well as decreased levels of T regulatory and myeloid suppressor cells within the tumor microenvironment. The preclinical data provide the rationale to design clinical trials with a combination of MUC1-based vaccine, celecoxib, and gemcitabine for the treatment of pancreatic cancer.

Pancreatic cancer is one of the leading causes of cancer-related deaths with a 5-year survival being <5% (1). Adjuvant therapies, which have undesirable side effects, have shown limited survival benefit, and very often the cancer becomes resistant to such therapies. Novel therapies such as cancer vaccines that target tumor associated Ags present an attractive alternative with the expectation that this approach will cause fewer side effects and prevent metastasis and recurrence better than standard therapies. Mucin-1 (MUC1)³ is one such tumor associated Ags (2).

¹This work is supported by research grants from the National Institutes of Health (R01 CA118944; P50 CA102701) and the American Association for Cancer Research/PanCan-Pilot Award.

Copyright © 2009 by The American Association of Immunologists, Inc. All rights reserved.

²Address correspondence and reprint requests to Dr. Pinku Mukherjee, Department of Biology, University of North Carolina, Charlotte, Woodward Hall, Charlotte, NC 28223. pmukherj@uncc.edu or mukherjee.pinku@mayo.edu.

Disclosures

The authors have no financial conflict of interest.

³Abbreviations used in this paper: MUC1, mucin-1; IHC, immunohistochemistry; TR, tandem repeat; COX-2, cyclooxygenase-2; MSC, myeloid suppressor; Treg, T regulatory cell; PDA, pancreatic ductal adenocarcinoma; Tg, transgenic; PanIN, pancreatic intraepithelial preneoplastic lesion; DC, dendritic cell; CIS, carcinoma in situ; TDLN, tumor draining lymph node.

MUC1 protein has been detected in >90% of pancreatic tumors examined by immunohistochemistry (IHC) (2, 3) and in the pancreatic juice of PDA patients by proteomic analysis, and in most pancreatic cancer cell lines (4, 5). Sialylated MUC1 is overexpressed by invading and metastatic pancreatic cancer cells but not by normal pancreas nor in cases of chronic pancreatitis or pancreatic ductal hyperplasia (6). MUC1 is a transmembrane mucin glycoprotein, which contains an extracellular domain comprised mainly of tandem repeats (TR) of twenty amino acids, a transmembrane domain, and a cytoplasmic tail. The core protein contains extensive *O*-glycosylation and MUC1 is highly expressed on the cell surface of many epithelial and hematologic malignancies (7–11). MUC1 on tumors is no longer restricted to the apical surface, but is found all around the cell surface and in the cytoplasm. In addition, glycosylation on tumor-synthesized MUC1 is aberrant (reviewed in Ref. 12 and 13). Thus, MUC1 has long been an interesting target molecule for immunotherapeutic strategies, given its highly increased expression and altered glycosylation in tumors (reviewed in Ref. 14). Patients with breast, pancreatic, and ovarian tumors have exhibited spontaneous immune responses to MUC1 with the presence of Abs and T cells specific for MUC1 (15–19).

Several clinical trials using the MUC1 TR region as the Ag have been described (20–25) (reviewed in Ref. 2, 26). Although tumor Ag-specific immune responses have been observed in cancer patients immunized with tumor Ag-based vaccines, they have rarely translated to a clinical response (recently reviewed in Ref. 27). Recent evidence has attributed this ineffectiveness to the immunosuppressive (also referred to as immunetolerant) tumor microenvironment which adapts numerous ways to resist killing by immune effector cells. Several factors have been implicated in this immunosuppression, one being cyclooxygenase-2 (COX-2) and its downstream prostaglandins (28–33). PGE₂ in particular, inhibits T effector cell activity and stimulates myeloid suppressor (MSCs) and T regulatory cells (Tregs) (34–37). In addition, it activates the IDO pathway that converts tryptophan to kynurenine and renders the tumor microenvironment low in tryptophan, an essential amino acid required by T effector cells to survive (38). We have previously shown that COX-2 inhibition significantly enhances the efficacy of a breast cancer vaccine by down regulating IDO function in a spontaneous metastatic breast cancer model (37). In addition, tumor cells treated with COX-2 siRNA inhibit the IDO enzymatic pathway (37), and in the COX-2 knockout mice, the IDO enzymatic activity is impaired (our unpublished data).

We have recently generated a triple transgenic (Tg) mouse model of pancreatic ductal adenocarcinoma (PDA) that expresses human MUC1 as a self molecule (39). We have crossed the LSL-KRAS^{G12D} × P⁴⁸Cre mouse developed by Hingorani et al. (40) with the human MUC1. Tg mice (41). These mice are designated PDA.MUC1 mice. This distinctive model of PDA expresses high levels of COX-2, IDO, and MUC1 and recapitulates the various stages of the human disease from preinvasive epithelial lesions (PanINs) to full blown adenocarcinoma (39). The PDA.MUC1 mice have increased circulating MUC1 and are tolerant to MUC1 immunization, making this model ideal for testing novel MUC1-based therapeutic strategies in combination with COX-2 inhibition.

In this study, we report that immunization with a MUC1-specific vaccine is only effective against pancreatic cancer if combined with celecoxib. By itself the vaccine is ineffective and so is celecoxib. Addition of a chemotherapeutic agent, gemcitabine at low doses, does not impair the immune effector cells elicited by the vaccine plus celecoxib. Clinically, this is reassuring because gemcitabine is a commonly used agent for pancreatic cancer patients and can be safely used in combination with the vaccine plus celecoxib without concern about its effect on immune effector cells. These findings support additional investigation of combination of vaccine, celecoxib, and gemcitabine for the treatment of pancreatic cancer in a human clinical trial.

Materials and Methods

Mice

The P48Cre expressing mice were bred to the LSL-KRAS^{G12D} mice (40) that were then mated to the human MUC1.Tg mice (designated PDA.MUC1 mice, Ref. 39) and were maintained as heterozygotes. Genomic DNA was used to genotype the triple transgenic mice using a PCR as previously described (39). All protocols were conducted in accordance with stringent regulations laid out by the Mayo Clinic Internal Animal Care and Use Committee (IACUC).

Treatment schedule and dose

The treatment schedule, dose, and route of administration are schematically represented in Fig. 1A. PDA.MUC1 mice were treated with the 1) vaccine, 2) vaccine plus celecoxib, 3) vaccine plus celecoxib plus gemcitabine, 4) celecoxib alone, and 5) vehicle. Gemcitabine was given 2 days before the vaccine every month starting at 4 mo of age. Mice were sacrificed between 9 and 10 mo of age and size of pancreas tumor evaluated by wet weight and used for histological evaluation of the PanIN lesions and adenocarcinoma. Serum was collected to determine levels of MUC1, anti-MUC1, PGE₂ metabolite, kynurenine, and tryptophan. Lymph nodes were dissected to determine anti-MUC1 cellular immune responses.

Evaluation and scoring of PanIN lesions and adenocarcinoma

The entire pancreas was dissected free of fat and surrounding tissue. Tissues were fixed and embedded in paraffin. Four-micrometer serial sections were cut and used and stained with H&E for counting the PanINs. PanINs were scored in five consecutive sections per pancreas and 10 fields per section.

Immunohistochemistry

The primary Abs used were goat anti-COX-2 mAb (1/100 dilution; Santa Cruz Biotechnology), goat anti-IDO mAb (1/50 dilution; Santa Cruz Biotechnology), mouse anti-PCNA mAb (5 µg/ml; BD Biosciences), rat anti-mouse FoxP3 mAb for staining Tregs (1/50 dilution; eBioscience), and rat anti-Gr-1 mAb for staining MSCs (1/100 dilution; BD Biosciences). Secondary Abs were anti-mouse (1/100; DakoCytomation), anti-hamster (1/250; The Jackson Laboratory), anti-goat (1/100; DakoCytomation), and anti-rat (DakoCytomation, 1/200 for MSCs and 1/100 for Tregs) IgGs conjugated to HRP. For TUNEL-positive cells, IHC was performed using the ApopTag Peroxidase in situ apoptosis detection kit (Serologicals). Sections were incubated overnight with the primary Ab followed by 1 h with secondary Ab and developed with a diaminobenzidine substrate (Vector Laboratories). Sections were counterstained with hematoxylin, and mounted with Permount. Immunopositivity was assessed using a light microscope and images taken at a magnification of ×100 or ×200.

ELISA for circulating levels of PGE₂ and anti-MUC1 Abs

PGE₂ levels in the serum was determined using a specific ELISA kit for PGE₂ metabolite (13,14-dihydro 15-keto prostaglandin A₂) (Cayman Pharmaceuticals) (37). Results are expressed as micrograms of PGE₂ metabolite/ml of serum. Serum MUC1 levels were determined using commercially available CA15–3 ELISA kit (Genway Biotech) (42). Detection of Ab to MUC1 was conducted by ELISA using synthetic peptides 105mer MUC1 TR as previously described (43).

Measurement of IDO activity by HPLC analysis of kynurenine and tryptophan

Using a published HPLC assay for IDO enzymatic activity measurement (44) as a starting point, we have optimized and validated a sensitive HPLC assay with UV and fluorescence detection that allows effective chromatographic separation of tryptophan and its metabolite kynurenine in serum.

IFN- γ ELISPOT

At time of sacrifice, cells from tumor draining lymph nodes (TDLNs) were isolated from treated PDA.MUC1 mice and used as responders in an IFN- γ ELISPOT assay. The stimulators were autologous bone-marrow derived dendritic cells (DCs) (37) pulsed with the immunizing peptides (20 $\mu\text{g}/\text{ml}$ of each peptide) for 2 h at 37°C. Following peptide stimulation, LPS (1 $\mu\text{g}/\text{ml}$; BD Biosciences) was added and incubated overnight to mature the DCs. DCs were analyzed by flow cytometry for appropriate maturation markers. The DCs were irradiated (7000 rad) using the RS 2000 irradiator (Rad Source Technologies). A responder (1×10^6 cells/ml) to stimulator (1×10^5 cells/ml) ratio of 10:1 was used. The responders and stimulators were incubated for 18 h on the ELISPOT plates before staining for the spots using the standard IFN- γ ELISPOT plates from Mabtech. MUC1-specific spots were determined using the capture IFN- γ Ab as recommended by the manufacturer. Control wells contained T cells stimulated with DCs pulsed with irrelevant peptide (vesicular stomatitis virus peptide, RGYKYQGL) or unpulsed DCs. Spot numbers were determined using computer assisted video image analysis by Zellnet Consulting. Splenocytes from C57BL/6 mice stimulated with Con A was used as positive control.

CTL assay

Determination of CTL activity was performed using a standard ^{51}Cr release method. Sorted T cells from TDLN served as effector cells. Autologous irradiated DCs pulsed with immunizing peptides (20 $\mu\text{g}/\text{ml}$) were used as stimulator cells and cocultured with the effector cells at a ratio of 10:1 for 18 h. Effector cells were incubated with ^{51}Cr -labeled tumor target cells at a ratio of 50:1 ($5 \times 10^6/\text{ml}$ effectors and $1 \times 10^5/\text{ml}$ targets). Target cells used were B16 melanoma cells expressing full-length human MUC1 (39, 43, 45, 46), and B16 melanoma cell line that does not express MUC1 as an irrelevant target. Radioactive ^{51}Cr released at the end of 6 h was determined using the Topcount Microscintillation Counter (Packard Biosciences). Specific lysis was calculated according to the following formula: $(\text{experimental cpms} - \text{spontaneous cpms}) / (\text{complete cpms} - \text{spontaneous cpms}) \times 100$. Spontaneous ^{51}Cr release in all experiments was 10–15% of complete ^{51}Cr release.

Statistical analysis

Biostatisticians at the Mayo Clinic Biostatistics Core Facility conducted statistical analysis for all data. A two-factor ANOVA was used to generate significant differences between experimental groups. For the ELISPOT analysis, data were adjusted for operator (different days at which assays were conducted).

Results

Immunization with MUC1-specific vaccine is effective only in combination with celecoxib

The treatment schedule, dose, and route of administration are schematically represented in Fig. 1A. As PDA.MUC1 mice age, they progressively develop PanINs and invasive adenocarcinomas (Fig. 1B). The progression of pancreatic tumors in PDA.MUC1 mice from 2 to 10 mo of age is shown in Fig. 1B signifying the rapid progression of PanINs to carcinoma in situ (CIS) and adenocarcinoma. Data from $n = 15$ mice are shown. PanIN

lesions were detected as early as 2 mo of age in ~50% of the mice and by 4 mo of age, 100% of the mice developed PanINs (Fig. 1B). By 6 mo of age, ~40% of the mice developed CIS and 25% developed invasive tumors, and by 9–10 mo of age, ~80–90% of the mice developed invasive adenocarcinomas (Fig. 1B). The MUC1 vaccine by itself was not effective in stopping the progression of PDA in the PDA.MUC1 mice (Fig. 2). This was indeed surprising because the same vaccine strategy was highly successful in preventing tumor formation in colon cancer models (45, 47). However, when the MUC1 vaccine was combined with a COX-2 inhibitor, its efficacy was significantly enhanced (Fig. 2). It must be noted that at time of sacrifice between 9 and 10 mo, ~85–100% of PDA.MUC1 mice have developed invasive adenocarcinoma (Fig. 1B). PDA.MUC1 mice treated with vaccine plus celecoxib or vaccine plus celecoxib plus gemcitabine showed significant decrease in pancreas weight compared with PDA.MUC1 mice treated with vehicle ($p < 0.001$), celecoxib ($p < 0.05$), or vaccine ($p < 0.01$) (Fig. 2A). The pancreas weight is used as the indicator of the tumor weight. Thus, the C57BL/6 pancreas weight represents the weight of a normal pancreas. Although significant decrease was observed in mice treated with celecoxib alone compared with vehicle ($p < 0.05$), the decrease was greater with the combination of vaccine and celecoxib with or without gemcitabine. There was no difference between vaccine and vehicle-treated mice. When PanIN lesions were counted, PanINs of all stages including PanIN 1, 2, and CIS was significantly lower in the mice treated with the combination of vaccine plus celecoxib \pm gemcitabine compared with mice treated with vehicle, celecoxib, or vaccine alone (Fig. 2B). The statistical differences between various experimental groups are illustrated in a form of a table within Fig. 2, clearly suggesting an advantage of the combination vs single-agent treatment. When numbers of mice that developed invasive adenocarcinoma were analyzed, out of $n = 15$ mice, none of the mice in the vaccine plus celecoxib \pm gemcitabine group developed adenocarcinoma whereas 11/15 in the vaccine group, 9/15 in the celecoxib group, and 13/15 in the vehicle group developed invasive adenocarcinomas (Fig. 2C). Representative H&E images shown in Fig. 3 accentuate the data showing the close to normal-looking pancreas from mice treated with the combination of vaccine plus celecoxib \pm gemcitabine. It is noteworthy that most of the pancreas sections seemed completely free of high-grade PanINs in mice treated with the combination. Average of $n = 15$ mice is presented. Note: Gemcitabine was titrated in these mice and toxicity (complete blood count and weight loss) recorded. The dose of 50 mg/kg once a month was selected based upon no change in complete blood count or weight and no effect on the tumor. The gemcitabine alone group was similar to the vehicle group and the gemcitabine plus vaccine group was similar to the vaccine group (data not shown).

Increased CTL activity in response to treatment with a combination of vaccine and celecoxib

At time of sacrifice, TDLNs were collected. T cells were sorted from the TDLNs into CD4⁺ and CD8⁺ T cells by MACS. IFN- γ ELISPOT and CTL assays were conducted. Significantly higher numbers of MUC1-specific IFN- γ -spot producing CD4⁺ and CD8⁺ cells were observed in vaccine plus celecoxib \pm gemcitabine group compared with vehicle, celecoxib, and vaccine treated mice (Fig. 4A). The appropriate controls for the ELISPOT assay are shown in a table form as part of Fig. 4A. Interestingly, vaccine-treated mice had higher spot-forming CD4⁺ T cells but not CD8⁺ T cells compared with vehicle and celecoxib while the mice treated with the combination (vaccine plus celecoxib) had higher CD8⁺ T effector response compared with vaccine alone. This was further corroborated with a robust CTL response against tumor targets expressing MUC1 in mice treated with the combination (Fig. 4B). Although multiple target cells were used, data is shown for the B16.MUC1 target cells. Similar results were noted when PDA.MUC1 cells were used as targets. This data is not included because we were unable to isolate PDA cell lines that lacked human MUC1 and therefore had no way to evaluate MUC1 specificity. The PDA

tumors without human MUC1 do not grow in vitro. The effector T cells were not lytic against the B16.neo or B16 wild-type cells suggesting that the lytic activity was specific to MUC1. Compared with the vehicle, all groups showed significantly increased ($p < 0.0001$) CTL activity, however the maximum killing was observed in the mice treated with the combination of vaccine plus celecoxib or vaccine plus celecoxib plus low-dose gemcitabine. This group showed significantly higher CTL activity compared with celecoxib alone or vaccine alone ($p < 0.0001$). No differences were observed between vaccine plus celecoxib and vaccine plus celecoxib plus gemcitabine groups. Vaccine alone showed significantly greater lytic activity compared with celecoxib alone ($p < 0.0001$). These data clearly suggest that the efficacy of vaccine or celecoxib alone is greatly enhanced by combining the two. Statistical analysis concluded that the effect of vaccine plus celecoxib was synergistic rather than additive.

Serum MUC1 and anti-MUC1 Ab levels in response to treatment

At time of sacrifice, serum was collected. Levels of serum MUC1 and anti-MUC1 Abs were evaluated post treatment by specific ELISAs. In brief, $n = 15$ mice were evaluated. Compared with mice treated with vehicle or celecoxib, a significant increase in anti-MUC1 Ab was observed in vaccine or vaccine plus celecoxib \pm gemcitabine-treated mice ($p < 0.0001$) (Fig. 4C). Taken together with the CTL data, the results suggest that the combination treatment elicits both a cellular and a humoral response against MUC1 that translates to an effective antitumor response. This could be important with regards to generating a sustained antitumor immune response. At the same time, when anti-MUC1 Ab levels increase, serum MUC1 levels decrease from ~ 1000 U/ml in the vehicle-treated mice to ~ 200 U/ml in the vaccine plus celecoxib \pm gemcitabine-treated mice (data not shown) suggesting that as tumor burden decreases so does MUC1 levels.

Repression of COX-2 and IDO enzymatic activities in response to celecoxib

We have recently published that addition of a COX-2 inhibitor to a DC-based breast cancer vaccine not only down-regulated the known COX-2 activity but also repressed IDO activity (37). We therefore determined if a similar phenomenon was observed in the PDA.MUC1 mice. Similar to our previous data, we show that inhibiting COX-2 down-regulates both the COX-2 and IDO expression of function in the treated tumors (Fig. 5). Representative sections from PDA.MUC1 tumors are shown for COX-2 and IDO expression from each treatment group (Fig. 5A). $n = 6$ mice were stained with similar results. Clearly, the expression of both COX-2 and IDO were lowest in tumors from mice treated with the combination of vaccine plus celecoxib \pm gemcitabine as compared with vehicle, vaccine alone, or celecoxib alone. The expression data in Fig. 5A matches the tumor burden data confirming absence of adenocarcinoma in mice treated with the combination of vaccine plus celecoxib \pm gemcitabine compared with either treatment alone (Figs. 2 and 3). It must be noted that we have not conducted any statistical analysis on the IHC data, but have done so for their respective enzymatic activity.

We show that down-regulation of protein expression was associated with decrease in their enzymatic activities (Fig. 5, B–D). Analysis of PGE₂ levels serves as the measure for COX-2 activity because COX-2 converts arachidonic acid to PGE₂. Similarly, kynurenine and tryptophan serve as a measure for IDO activity because IDO converts tryptophan to kynurenine. In tumor-bearing mice, IDO and COX-2 activity are high and therefore PGE₂ and kynurenine levels are high while tryptophan levels are low (39). As tumor burden decreases (with treatment), we expect that levels of PGE₂ and kynurenine would decline and tryptophan levels would increase. This is exactly what we observe and report in Fig. 5, B–D. As expected, all experimental groups of mice expressed significantly higher levels of circulating PGE₂ compared with the control C57BL/6 serum (Fig. 5B, $p < 0.001$). With

treatment, significant decrease in PGE₂ levels was observed in mice treated with celecoxib alone or celecoxib plus vaccine ± gemcitabine ($p < 0.01$) compared with vehicle or vaccine alone. However, the levels never came down to nontumor-bearing C57BL/6 levels, suggesting presence of residual COX-2 activity. There was no change between mice treated with vaccine and vehicle. Average of $n = 15$ mice are shown (Fig. 5B). Using a modified HPLC method, serum levels of tryptophan and kynurenine was determined (Fig. 5, C and D). As predicted, significantly lower tryptophan levels were observed in serum of tumor-bearing PDA.MUC1 mice treated with vehicle compared with serum from a nontumor-bearing C57BL/6 mice (Fig. 5C, $p = 0.001$). When PDA.MUC1 mice were treated with celecoxib or celecoxib plus vaccine ± gemcitabine, tryptophan levels significantly increased to levels similar to the nontumor-bearing C57BL/6 mice (Fig. 5C, $p = 0.002$, $p = 0.05$, and $p = 0.01$, respectively, compared with vehicle-treated mice), suggesting that celecoxib treatment with or without the vaccine inhibited IDO activity. No significant difference was noted between nontumor-bearing C57BL/6 mice, celecoxib-treated or celecoxib plus vaccine ± gemcitabine-treated PDA.MUC1 mice. Vaccine treatment by itself had no effect on the tryptophan levels and the levels remained similar to vehicle-treated mice (Fig. 5C). Low tryptophan represents high IDO activity because IDO converts tryptophan to kynurenine. Thus, it was not unexpected to observe significantly higher levels of kynurenine in sera of PDA.MUC1 mice belonging to the vehicle-treated group compared with the nontumor bearing C57BL/6 mice (Fig. 5D, $p = 0.0001$). These levels decreased significantly when mice were treated with celecoxib or celecoxib plus vaccine ± gemcitabine (Fig. 5D; $p = 0.05$, $p = 0.05$, and $p = 0.001$, respectively), clearly suggesting down-regulation of IDO activity with celecoxib treatment. Vaccine alone had no effect on the kynurenine levels (Fig. 5D). Lysates from the tumor were also tested for PGE₂, kynurenine, and tryptophan levels. The data followed a similar trend as noted with the serum (data not shown). We suggest that inhibiting COX-2 decreases IDO function and enables the effector T cells (CTLs) to be active within the pancreatic tumor microenvironment.

Decreased Tregs and MSCs in the pancreatic tumor microenvironment in response to the combination treatment

Several reports implicate COX-2/PGE₂ and IDO in the increased recruitment of Tregs and MSCs to the tumor microenvironment and causing T effector cell apoptosis (34–37, 48–50). We therefore examined if the combination treatment altered the levels of FoxP3⁺ and Gr1⁺ cells in the tumor microenvironment by IHC. We have previously shown by quantitative flow cytometry that tumors from 9 to 10 mo old PDA.MUC1 mice encompass high levels of Tregs and MSCs (39). In accordance with previous results, we observed high levels of FoxP3⁺ and Gr-1⁺ cells (by IHC) within the PDA.MUC1 tumors that were treated with vehicle (Fig. 6, A and B). However, the levels declined appreciably in tumors treated with the combination of vaccine plus celecoxib ± gemcitabine (Fig. 6, A and B). Single treatment with vaccine or celecoxib alone did not alter the levels of these cells. Ten fields in five consecutive pancreas tumor sections from $n = 4$ mice per group were evaluated. Due to the diffuse nature of staining, positive cells were not scored and statistical analysis was not conducted. Nevertheless, there was a clear decrease in these cell types in tumors treated with the combination. One representative image from each group is shown. These data suggest that the high systemic and local proinflammatory environment in the PDA.MUC1 mice can be reversed by the combination treatment and can lead to a significant clinical response.

Increased in situ apoptosis and decreased proliferation in response to the combination treatment

Using an in situ TUNEL assay, we determined if the tumors from mice treated with the combination of vaccine and celecoxib had significantly higher numbers of apoptotic cells compared with mice treated with either agent alone or vehicle (Fig. 6C). The number of

positive cells was scored across ten fields in five consecutive pancreas tumor sections for $n = 4$ mice per group and they were as follows: vehicle: 150 ± 102 ; celecoxib: 650 ± 102 ; vaccine: 392 ± 112 ; vaccine \pm celecoxib: 1250 ± 214 ; vaccine \pm celecoxib \pm gemcitabine: 1575 ± 245 . Compared with vehicle, TUNEL-positive cells were significantly greater in all treatment groups including celecoxib ($p < 0.04$), vaccine ($p = 0.06$), vaccine plus celecoxib ($p < 0.001$), and vaccine plus celecoxib plus gemcitabine ($p < 0.001$, compared with vehicle-treated mice), however, the combination of vaccine plus celecoxib \pm gemcitabine showed appreciably higher TUNEL-positive cells compared with either treatment alone ($p < 0.01$). As predicted, proliferation was significantly lower in the tumors of mice treated with the combination of vaccine plus celecoxib \pm gemcitabine compared with mice treated with vehicle or single agent alone (Fig. 6D). When PCNA-positive cells were scored, we found no significant difference in the PCNA⁺ cell numbers between vehicle (460 ± 70), celecoxib (520 ± 85), and vaccine (440 ± 90) groups. However, PCNA⁺ cells in tumors treated with the combination of vaccine plus celecoxib (5 ± 2), or vaccine plus celecoxib plus gemcitabine (3 ± 2) was significantly lower than in vehicle-treated or single agent-treated tumors (0.0001).

Discussion

With the development of early pancreatic tumors in mouse models and identification of immune-system regulatory signaling pathways, new opportunities for pancreas cancer treatment and prevention have emerged. Immunotherapy for pancreatic cancer is one approach that may greatly benefit from these discoveries, as therapeutics can be developed to target pancreatic cancer-associated Ags and regulatory signaling molecules.

In a novel mouse model of spontaneous PDA that expresses human MUC1 as a self molecule, we demonstrate that overcoming immunosuppression by blocking the COX-2 pathway during pancreatic cancer development significantly enhances the clinical efficacy of a MUC1-targeted vaccine. The MUC1-vaccine by itself was completely ineffective in stopping progression of PDA (Fig. 2), albeit did elicit a strong anti-MUC1 immune response (Fig. 4), with results similar to reports from several human immunotherapy trials (51). However, this was a bit surprising because the same vaccine was shown by our own group to be highly effective in MUC1-tolerant colon cancer model (45, 47). Other vaccine strategy such as DC pulsed with the MUC1 peptides as well as DC pulsed with tumor lysate has been tested without success in this model (data not shown). The results exemplify the importance of the PDA.MUC1 model in which the tumors arise spontaneously within the appropriate stromal and hormonal milieu. We have shown that the pancreas tumors in PDA.MUC1 mice express high levels of COX-2 and are highly immunosuppressed (39). Thus, when COX-2 inhibition was introduced at 4 mo of age after the mice had received two monthly immunizations with the MUC1 vaccine (Fig. 1A), the antitumor effect was overwhelming (Figs. 2 and 3) with none of the mice developing adenocarcinoma. Although blocking COX-2 alone without the vaccine had some effect on the development of PanIN lesions compared with vehicle-treated mice (Fig. 2B), nine of fifteen mice progressed to develop adenocarcinomas (Fig. 2C). Both anti-MUC1 CTL and Ab responses were enhanced with the combination treatment (Fig. 4) leading to a robust clinical response. We attribute this robust CTL response not only to the down-regulation of PGE₂ but also to the diminished IDO function, which led to higher tryptophan levels (that is known to support T effector cell survival and function) (Fig. 5). In addition, infiltration of Tregs (FoxP3⁺ cells) and MSCs (Gr-1⁺ cells) within the tumor bed was virtually nonexistent in tumors from mice treated with the combination (Fig. 6, A and B). The clinical efficacy of the treatment regimen was further supported by the enhanced apoptosis in the tumor alongside decreased proliferation (Fig. 6, C and D). These data once again point to the regulation of IDO expression and function by inhibition of the COX-2/PGE₂ pathway as previously reported (37). The

proinflammatory microenvironment in the PDA.MUC1 mice which normally expresses high PGE₂, kynurenine, MUC1, Tregs, and MSCs was completely reversed by the combination treatment leading to low proliferation in the tumor (Figs. 5 and 6). We recognize that the downstream effects on Tregs and MSCs may be driven by the low tumor burden in the mice treated with the combination, nevertheless, the robust clinical and immunologic response with the combination warrants future evaluation in a clinical setting.

Importantly, the efficacy of the immune responses elicited by the combination treatment (vaccine plus celecoxib) was not diminished by the addition of low-dose gemcitabine to the treatment regimen (Fig. 4), suggesting that the dose and schedule of the chemotherapy was not deleterious to the immune effector cells. This data could be significant while designing future clinical trials for pancreatic cancer patients. Surprisingly, however, we did not observe any significant clinical improvement in mice treated with all three agents (vaccine plus celecoxib plus gemcitabine) over mice treated with the two agents (celecoxib plus vaccine). Low-dose gemcitabine plus vaccine did not show any clinical efficacy and was similar to vaccine alone group (data not shown). This is possibly due to the low-dose of gemcitabine used once a month which by itself had no effect on the tumor nor caused any toxicity (data not shown). The rationale for including gemcitabine to the treatment regimen was simply to test if low-dose chemotherapy given two days before the vaccine could enhance effector T cell function by inhibiting Tregs as reported for other chemotherapeutic agents such as cyclophosphamide (52, 53). In our study, gemcitabine did not show a change in T effector cells or Tregs compared with vaccine plus celecoxib (Fig. 4 and 6). In most instances the vaccine plus celecoxib and vaccine plus celecoxib plus gemcitabine groups were similar.

It must be noted that these experiments were conducted in a semiprophyllactic²/semitherapeutic setting with immunizations beginning at 2 mo of age, at which time the pancreas in the PDA.MUC1 mice have only low-grade PanIN lesions (Fig. 1B and Ref. 39). The celecoxib and gemcitabine treatment was started at a later time at 4 mo of age when high-grade PanINs and CIS were rampant in these mice (39). Other experimental controls ($n = 5$ mice) that were included in the study but data not shown were 1) gemcitabine alone (results were similar to vehicle), 2) celecoxib plus gemcitabine (results were similar to celecoxib alone group), and 3) vaccine plus gemcitabine (results similar to vaccine alone group). We have now started these studies in a therapeutic setting with all treatments including the vaccine starting at 4 mo of age.

Another question that remains is how the combination of the three agents affects long-term survival in these mice. In a very preliminary study, five mice that received all three agents were allowed to survive beyond 40-wk of age. Vaccine and gemcitabine was discontinued at 8 mo of age. Celecoxib was continued as daily gavage. These mice lived for >16 mo of age without signs of morbidity (data not shown). Two of the five mice developed adenocarcinoma and the other three had high-grade PanIN lesions (data not shown). It should be noted that untreated PDA.MUC1 mice are morbid by 10–12 mo of age due to the pancreas tumor burden and weight loss. These preliminary studies are enticing and warrant further studies with more mice. Because these are triple transgenic mice, the generation of enough mice to reach statistical significance has been the challenge for completing the survival experiments. Currently, mice are being randomized into these long-term studies.

With the growing understanding of the regulation of immune responses, multiple new immunotherapeutic targets have evolved. Although several trials have shown detectable immune responses, such as delayed-type hypersensitivity reactions, and cytokine release in ELISPOT assays, and some have reported prolonged survival for immune responders, immunotherapy for pancreatic cancer remains experimental. However, some approaches

have made it to phase III settings (27). In a recent report, use of cyclophosphamide 1 day before whole tumor cell vaccine was well tolerated by advanced pancreatic cancer patients and generated mesothelin-specific T cells responses. In addition, chemotherapy plus immunotherapy resulted in median survival in a gemcitabine-resistant population similar to chemotherapy alone (54), thus supporting additional investigation of chemotherapy with immunotherapy in patients with advanced pancreatic cancer.

This is the first report in a mouse model that the combination of immunotherapy and COX-2 inhibition with or without gemcitabine may be an effective therapy for pancreas cancer. We cannot overemphasize that the mouse model used in these studies mimics the human disease with the tumors arising in an immune competent host and progressing from PanIN lesions to CIS to full-blown invasive adenocarcinomas (39, 40, 46). The fact that the vaccination is conducted in a MUC1-tolerant host makes it an even better study and closer to the human situation.

The data presented in this study exemplifies the importance of 1) an appropriate tumor model system, 2) targeting a pancreatic tumor-associated Ag, namely MUC1, and 3) the critical role of COX-2/PGE₂ pathway in modulating the proinflammatory tumor microenvironment which is highly immunosuppressive.

Acknowledgments

We thank Dr. Sandra Gendler for gifting the MUC1.Tg mice and the MUC1-specific Abs as well as for her critical comments; Dr. Tyler Jacks and Chris Wright for their willingness to discuss and share the LSL-KRasG12D and P24-Cre mice; our pathologists, Dr. R. Marler, for his critical comments on the histology slides; August J. Klug for his contribution on maintaining and genotyping the PDA.MUC1 mice; all members in the animal, histology, and biostatistics cores; Nichole Boruff in the Visual Communications Core for her help with the preparation of the figures; and Irene Beauvais for her help in submitting this manuscript.

References

1. Jemal A, Murray T, Ward E, Samuels A, Tiwari RC, Ghafoor A, Feuer EJ, Thun MJ. Cancer statistics, 2005. *CA Cancer J Clin.* 2005; 55:10–30. [PubMed: 15661684]
2. Plate JM, Shott S, Harris JE. Immunoregulation in pancreatic cancer patients. *Cancer Immunol Immunother.* 1999; 48:270–279. [PubMed: 10478644]
3. Qu CF, Li Y, Song YJ, Rizvi SM, Raja C, Zhang D, Samra J, Smith R, Perkins AC, Apostolidis C, Allen BJ. MUC1 expression in primary and metastatic pancreatic cancer cells for in vitro treatment by (213)Bi-C595 radioimmunoconjugate. *Br J Cancer.* 2004; 91:2086–2093. [PubMed: 15599383]
4. Gronborg M, Bunkenborg J, Kristiansen TZ, Jensen ON, Yeo CJ, Hruban RH, Maitra A, Goggins MG, Pandey A. Comprehensive proteomic analysis of human pancreatic juice. *J Proteome Res.* 2004; 3:1042–1055. [PubMed: 15473694]
5. Hollingsworth MA, Strawhecker JM, Caffrey TC, Mack DR. Expression of MUC1, MUC2, MUC3 and MUC4 mucin mRNAs in human pancreatic and intestinal tumor cell lines. *Int J Cancer.* 1994; 57:198–203. [PubMed: 8157358]
6. Masaki Y, Oka M, Ogura Y, Ueno T, Nishihara K, Tangoku A, Takahashi M, Yamamoto M, Irimura T. Sialylated MUC1 mucin expression in normal pancreas, benign pancreatic lesions, and pancreatic ductal adenocarcinoma. *Hepatogastroenterology.* 1999; 46:2240–2245. [PubMed: 10521973]
7. Zotter S, Hageman PC, Lossnitzer A, Mooi WJ, Hilgers J. Tissue and tumor distribution of human polymorphic epithelial mucin. *Cancer Rev.* 1988; 11–12:55–101.
8. Girling A, Bartkova J, Burchell J, Gendler S, Gillet C, Taylor-Papadimitriou J. A core protein epitope of the polymorphic epithelial mucin detected by the monoclonal antibody SM-3 is selectively exposed in a range of primary carcinomas. *Int J Cancer.* 1989; 43:1072–1076. [PubMed: 2471698]

9. Croce MV, Isla-Larrain MT, Rua CE, Rabassa ME, Gendler SJ, Segal-Eiras A. Patterns of MUC1 tissue expression defined by an anti-MUC1 cytoplasmic tail monoclonal antibody in breast cancer. *J Histochem Cytochem.* 2003; 51:781–788. [PubMed: 12754289]
10. Treon SP, Mollick JA, Urashima M, Teoh G, Chauhan D, Ogata A, Raje N, Hilgers JHM, Nadler L, Belch AR, et al. MUC1 core protein is expressed on multiple myeloma cells and is induced by dexamethasone. *Blood.* 1999; 93:1287–1298. [PubMed: 9949172]
11. Brossart P, Schneider A, Dill P, Schammann T, Grunebach F, Wirths S, Kanz L, Buhning HJ, Brugger W. The epithelial tumor antigen MUC1 is expressed in hematological malignancies and is recognized by MUC1-specific cytotoxic T-lymphocytes. *Cancer Res.* 2001; 61:6846–6850. [PubMed: 11559560]
12. Gendler SJ. MUC1, the renaissance molecule. *J Mammary Gland Biol Neoplasia.* 2001; 6:339–353. [PubMed: 11547902]
13. Hanisch FG, Muller S. MUC1: the polymorphic appearance of a human mucin. *Glycobiology.* 2000; 10:439–449. [PubMed: 10764832]
14. Acres B, Limacher JM. MUC1 as a target antigen for cancer immunotherapy. *Expert Rev Vaccines.* 2005; 4:493–502. [PubMed: 16117706]
15. Barnd DL, Lan MS, Metzgar RS, Finn OJ. Specific, major histocompatibility complex-unrestricted recognition of tumor-associated mucins by human cytotoxic T cells. *Proc Natl Acad Sci USA.* 1989; 86:7159–7163. [PubMed: 2674949]
16. Ioannides CG, Fisk B, Jerome KR, Irimura T, Wharton JT, Finn OJ. Cytotoxic T cells from ovarian malignant tumors can recognize polymorphic epithelial mucin core peptides. *J Immunol.* 1993; 151:3693–3703. [PubMed: 7690810]
17. Jerome KR, Domenech N, Finn OJ. Tumor-specific cytotoxic T cell clones from patients with breast and pancreatic adenocarcinoma recognize EBV-immortalized B cells transfected with polymorphic epithelial mucin complementary DNA. *J Immunol.* 1993; 151:1654–1662. [PubMed: 8393050]
18. Rughetti A, Turchi V, Ghetti CA, Scambia G, Panici PB, Roncucci G, Mancuso S, Frati L, Nuti M. Human B-cell immune response to the polymorphic epithelial mucin. *Cancer Res.* 1993; 53:2457–2459. [PubMed: 8495404]
19. Kotera Y, Fontenot JD, Pecher G, Metzgar RS, Finn OJ. Humoral immunity against a tandem repeat epitope of human mucin MUC-1 in sera from breast, pancreatic, and colon cancer patients. *Cancer Res.* 1994; 54:2856–2860. [PubMed: 7514493]
20. Apostolopoulos V, Pietersz GA, Tsibanis A, Tsikkinis A, Drakaki H, Loveland BE, Piddlesden SJ, Plebanski M, Pouniotis DS, Alexis MN, et al. Pilot phase III immunotherapy study in early-stage breast cancer patients using oxidized mannan-MUC1 [ISRCTN71711835]. *Breast Cancer Res.* 2006; 8:R27. [PubMed: 16776849]
21. Wierecky J, Muller MR, Wirths S, Halder-Oehler E, Dorfel D, Schmidt SM, Hantschel M, Brugger W, Schroder S, Horger MS, et al. Immunologic and clinical responses after vaccinations with peptide-pulsed dendritic cells in metastatic renal cancer patients. *Cancer Res.* 2006; 66:5910–5918. [PubMed: 16740731]
22. North S, Butts C. Vaccination with BLP25 liposome vaccine to treat non-small cell lung and prostate cancers. *Expert Rev Vaccines.* 2005; 4:249–257. [PubMed: 16026241]
23. North SA, Graham K, Bodnar D, Venner P. A pilot study of the liposomal MUC1 vaccine BLP25 in prostate specific antigen failures after radical prostatectomy. *J Urol.* 2006; 176:91–95. [PubMed: 16753376]
24. Ramanathan RK, Lee KM, McKolanis J, Hitbold E, Schraut W, Moser AJ, Warnick E, Whiteside T, Osborne J, Kim H, et al. Phase I study of a MUC1 vaccine composed of different doses of MUC1 peptide with SB-AS2 adjuvant in resected and locally advanced pancreatic cancer. *Cancer Immunol Immunother.* 2005; 54:254–264. [PubMed: 15372205]
25. Loveland BE, Zhao A, White S, Gan H, Hamilton K, Xing PX, Pietersz GA, Apostolopoulos V, Vaughan H, Karanikas V, et al. Mannan-MUC1-pulsed dendritic cell immunotherapy: a phase I trial in patients with adenocarcinoma. *Clin Cancer Res.* 2006; 12:869–877. [PubMed: 16467101]
26. Schlom J, Arlen PM, Gulley JL. Cancer vaccines: moving beyond current paradigms. *Clin Cancer Res.* 2007; 13:3776–3782. [PubMed: 17606707]

27. Stielor J. Immunotherapeutic approaches in pancreatic cancer. *Recent Results Cancer Res.* 2008; 177:165–177. [PubMed: 18084958]
28. Coussens LM, Werb Z. Inflammation and cancer. *Nature.* 2002; 420:860–867. [PubMed: 12490959]
29. Juuti A, Louhimo J, Nordling S, Ristimaki A, Haglund C. Cyclo-oxygenase-2 expression correlates with poor prognosis in pancreatic cancer. *J Clin Pathol.* 2006; 59:382–386. [PubMed: 16467169]
30. Okuno K, Jinnai H, Lee YS, Nakamura K, Hirohata T, Shigeoka H, Yasutomi M. A high level of prostaglandin E₂ (PGE₂) in the portal vein suppresses liver-associated immunity and promotes liver metastases. *Surg Today.* 1995; 25:954–958. [PubMed: 8640020]
31. Sharma S, Stolina M, Yang SC, Baratelli F, Lin JF, Atianzar K, Luo J, Zhu L, Lin Y, Huang M, et al. Tumor cyclooxygenase 2-dependent suppression of dendritic cell function. *Clin Cancer Res.* 2003; 9:961–968. [PubMed: 12631593]
32. Lang S, Picu A, Hofmann T, Andratschke M, Mack B, Moosmann A, Gires O, Tiwari S, Zeidler R. COX-inhibitors relieve the immunosuppressive effect of tumor cells and improve functions of immune effectors. *Int J Immunopathol Pharmacol.* 2006; 19:409–419. [PubMed: 16831307]
33. Iwamoto A, Ikeguchi M, Matsumoto S, Hukumoto Y, Inoue M, Ozaki T, Ataka M, Tanida T, Endo K, Katano K, Hirooka Y. Tumor cyclo-oxygenase-2 gene suppresses local immune responses in patients with hepatocellular carcinoma. *Tumori.* 2006; 92:130–133. [PubMed: 16724692]
34. Jarnicki AG, Lysaght J, Todryk S, Mills KH. Suppression of antitumor immunity by IL-10 and TGF- β -producing T cells infiltrating the growing tumor: influence of tumor environment on the induction of CD4⁺ and CD8⁺ regulatory T cells. *J Immunol.* 2006; 177:896–904. [PubMed: 16818744]
35. Sharma S, Yang SC, Zhu L, Reckamp K, Gardner B, Baratelli F, Huang M, Batra RK, Dubinett SM. Tumor cyclooxygenase-2/prostaglandin E₂-dependent promotion of FOXP3 expression and CD4⁺ CD25⁺ T regulatory cell activities in lung cancer. *Cancer Res.* 2005; 65:5211–5220. [PubMed: 15958566]
36. Von Bergwelt-Baildon MS, Popov A, Saric T, Chemnitz JM, Classen S, Stoffel MS, Fiore F, Roth U, Beyer M, Debey S, Wickenhauser C, Hanisch FG, Schultze JL. CD25 and indoleamine 2,3-dioxygenase are upregulated by prostaglandin E₂ and expressed by tumor-associated dendritic cells in vivo: additional mechanisms of T cell inhibition. *Blood.* 2006; 108:228–237. [PubMed: 16522817]
37. Basu GD, Tinder TL, Bradley JM, Tu T, Hattrup CL, Pockaj BA, Mukherjee P. Cyclooxygenase-2 inhibitor enhances the efficacy of a breast cancer vaccine: role of IDO. *J Immunol.* 2006; 177:2391–2402. [PubMed: 16888001]
38. Uyttenhove C, Pilotte L, Theate I, Stroobant V, Colau D, Parmentier N, Boon T, Van den Eynde BJ. Evidence for a tumoral immune resistance mechanism based on tryptophan degradation by indoleamine 2,3-dioxygenase. *Nat Med.* 2003; 9:1269–1274. [PubMed: 14502282]
39. Tinder TL, Subramani DB, Basu GD, Bradley JM, Schettini J, Million A, Skaar T, Mukherjee P. MUC1 enhances tumor progression and contributes toward immunosuppression in a mouse model of spontaneous pancreatic adenocarcinoma. *J Immunol.* 2008; 181:3116–3125. [PubMed: 18713982]
40. Hingorani SR, Petricoin EF III, Maitra A, Rajapaske V, King C, Jacobetz MA, Ross S, Conrads TP, Veenstra TD, Hitt BA, et al. Preinvasive and invasive ductal pancreatic cancer and its early detection in the mouse. *Cancer Cell.* 2003; 4:437–450. [PubMed: 14706336]
41. Rowse GJ, Tempero RM, VanLith ML, Hollingsworth MA, Gendler SJ. Tolerance and immunity to MUC1 in a human MUC1 transgenic murine model. *Cancer Res.* 1998; 58:315–321. [PubMed: 9443411]
42. Gion M, Mione R, Leon AE, Dittadi R. Comparison of the diagnostic accuracy of CA27.29 and CA15.3 in primary breast cancer. *Clin Chem.* 1999; 45:630–637. [PubMed: 10222349]
43. Mukherjee P, Ginardi AR, Madsen CS, Sterner CJ, Adriance MC, Tevethia MJ, Gendler SJ. Mice with spontaneous pancreatic cancer naturally develop MUC1-specific CTLs that eradicate tumors when adoptively transferred. *J Immunol.* 2000; 165:3451–3460. [PubMed: 10975866]

44. Torres MI, Lopez-Casado MA, Lorite P, Rios A. Tryptophan metabolism and indoleamine 2,3-dioxygenase expression in coeliac disease. *Clin Exp Immunol*. 2007; 148:419–424. [PubMed: 17362267]
45. Mukherjee P, Pathangey LB, Bradley JB, Tinder TL, Basu GD, Akporiaye ET, Gendler SJ. MUC1-specific immune therapy generates a strong anti-tumor response in a MUC1-tolerant colon cancer model. *Vaccine*. 2007; 25:1607–1618. [PubMed: 17166639]
46. Tinder TL, Subramani DB, Basu GD, Bradley JM, Schettini J, Million A, Skaar T, Mukherjee P. MUC1 enhances tumor progression and contributes towards immunosuppression in a mouse model of spontaneous pancreatic adenocarcinoma. *J Immunol*. 2008; 181:3116–3125. [PubMed: 18713982]
47. Akporiaye ET, Bradley-Dunlop D, Gendler SJ, Mukherjee P, Madsen CS, Hahn T, Besselsen DG, Dial SM, Cui H, Trevor K. Characterization of the MUC1.Tg/MIN transgenic mouse as a model for studying antigen-specific immunotherapy of adenomas. *Vaccine*. 2007; 25:6965–6974. [PubMed: 17707958]
48. Muller AJ, Scherle PA. Targeting the mechanisms of tumoral immune tolerance with small-molecule inhibitors. *Nat Rev Cancer*. 2006; 6:613–625. [PubMed: 16862192]
49. Munn DH. Indoleamine 2,3-dioxygenase, tumor-induced tolerance and counter-regulation. *Curr Opin Immunol*. 2006; 18:220–225. [PubMed: 16460921]
50. Munn DH, Mellor AL, Rossi M, Young JW. Dendritic cells have the option to express IDO-mediated suppression or not. *Blood*. 2005; 105:2618. [PubMed: 15746089]
51. Plate JM. Current immunotherapeutic strategies in pancreatic cancer. *Surg Oncol Clin North Am*. 2007; 16:919–943. xi.
52. Thomas AM, Santarsiero LM, Lutz ER, Armstrong TD, Chen YC, Huang LQ, Laheru DA, Goggins M, Hruban RH, Jaffee EM. Mesothelin-specific CD8⁺ T cell responses provide evidence of in vivo cross-priming by antigen-presenting cells in vaccinated pancreatic cancer patients. *J Exp Med*. 2004; 200:297–306. [PubMed: 15289501]
53. Ercolini AM, Ladle BH, Manning EA, Pfannenstiel LW, Armstrong TD, Machiels JP, Bieler JG, Emens LA, Reilly RT, Jaffee EM. Recruitment of latent pools of high-avidity CD8⁺ T cells to the antitumor immune response. *J Exp Med*. 2005; 201:1591–1602. [PubMed: 15883172]
54. Laheru D, Lutz E, Burke J, Biedrzycki B, Solt S, Onners B, Tartakovsky I, Nemunaitis J, Le D, Sugar E, et al. Allogeneic granulocyte macrophage colony-stimulating factor-secreting tumor immunotherapy alone or in sequence with cyclophosphamide for metastatic pancreatic cancer: a pilot study of safety, feasibility, and immune activation. *Clin Cancer Res*. 2008; 14:1455–1463. [PubMed: 18316569]

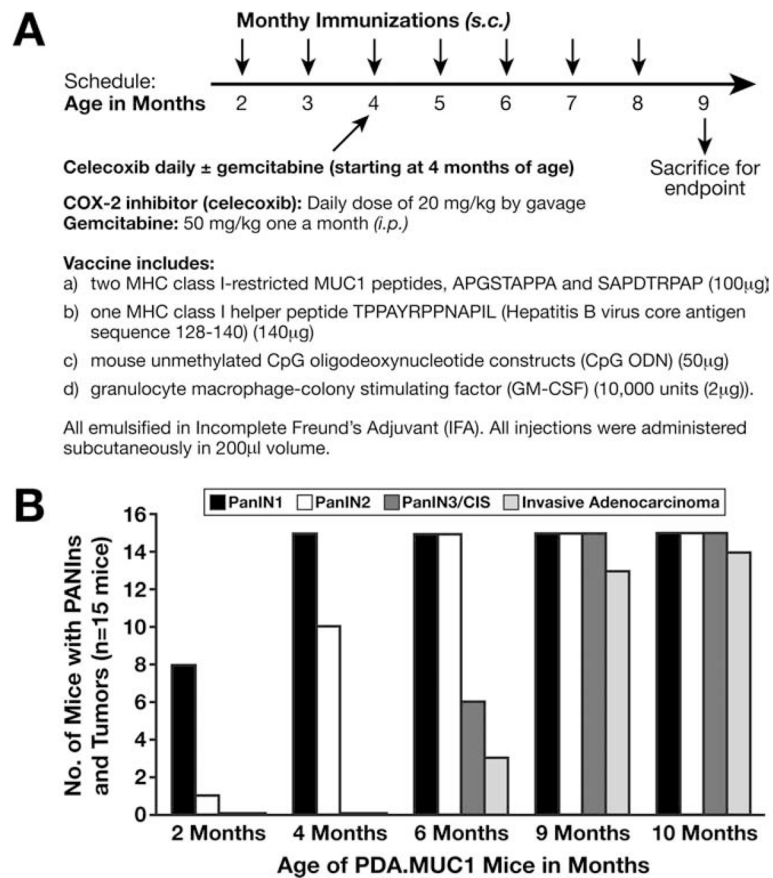
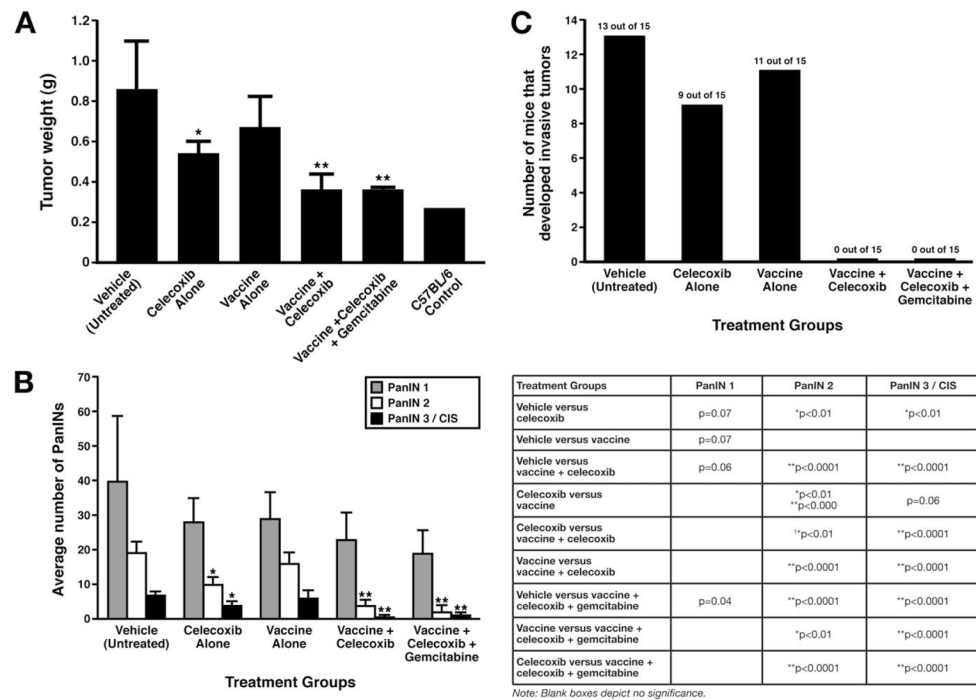


FIGURE 1.

A, Schematic representation of the treatment protocol and *B*, Progression of PanINs to invasive carcinoma as a function of age. Number of PDA.MUC1 mice that developed PanINs and adenocarcinomas of 15 mice evaluated.

**FIGURE 2.**

Immunization with MUC1-specific vaccine in combination with celecoxib \pm gemcitabine significantly reduces pancreatic cancer development in PDA.MUC1 mice. **A**, Pancreas wet weight at time of sacrifice (9 mo of age) for each treatment group; $n = 15$ mice per treatment group. *, $p < 0.05$; **, $p < 0.01$ compared with vehicle. **B**, Average number of PanINs in five consecutive sections and ten fields per section; $n = 15$ mice, p values between treatment groups are listed in the table. **C**, Numbers of mice (of 15 per treatment group) that develop invasive adenocarcinoma. Note: The wet weight of a normal pancreas from a nontumor bearing C57BL/6 mice is shown for comparison.

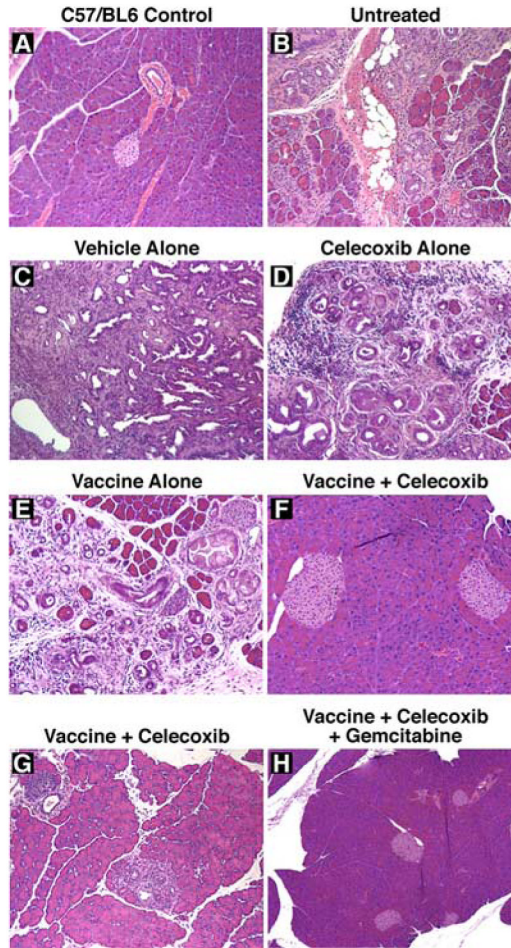
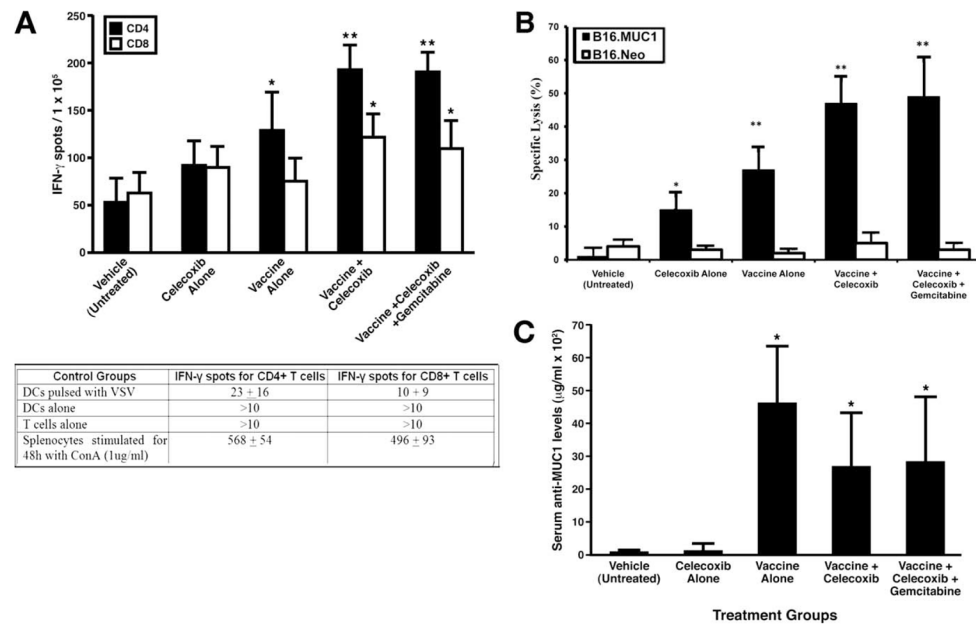


FIGURE 3.

Normal-looking pancreas in PDA.MUC1 mice treated with a combination of MUC1-vaccine plus celecoxib \pm gemcitabine. Representative histopathology (H&E) images of pancreas from normal C57BL/6 (A), untreated (B), vehicle (C), celecoxib (D), vaccine (E), vaccine plus celecoxib (F), and vaccine plus celecoxib plus gemcitabine-treated PDA.MUC1 mice (G and H). Pancreas from the PDA.MUC1 mice was dissected at time of sacrifice (9 mo of age). Age-matched nontumor-bearing C57BL/6 pancreas was used as control. PDA.MUC1 mice were treated as shown in Fig. 1A. $n = 15$ mice per group. Images were captured at $\times 200$ magnification.

**FIGURE 4.**

Treatment with the combination of vaccine plus celecoxib \pm gemcitabine elicits a strong cellular and humoral anti-MUC1 immune response in PDA.MUC1 mice. *A*, Sorted CD4⁺ and CD8⁺ T cells from TDLNs were assessed for IFN- γ production in response to the immunizing MUC1 peptides by ELISPOT assay. The table shows the controls that were used to confirm specificity of the response to the immunizing peptides. Average of $n = 15$ mice are shown. *, $p < 0.05$; **, $p < 0.01$ compared with vehicle-treated mice. *B*, Determination of CTL activity was performed using a standard ⁵¹Cr-release method. Sorted CD8⁺ T cells from TDLNs served as effector cells, autologous irradiated DCs pulsed with the immunizing peptides were used as stimulator cells and targets were B16.MUC1 or B16.Neo cells. Average of $n = 15$ mice are shown. *, $p < 0.001$ and **, $p < 0.0001$ as compared with vehicle-treated mice. *C*, Circulating levels of anti-MUC1 Ab levels was determined by ELISA. Average of $n = 15$ mice are shown. *, $p < 0.0001$ as compared with vehicle-treated mice.

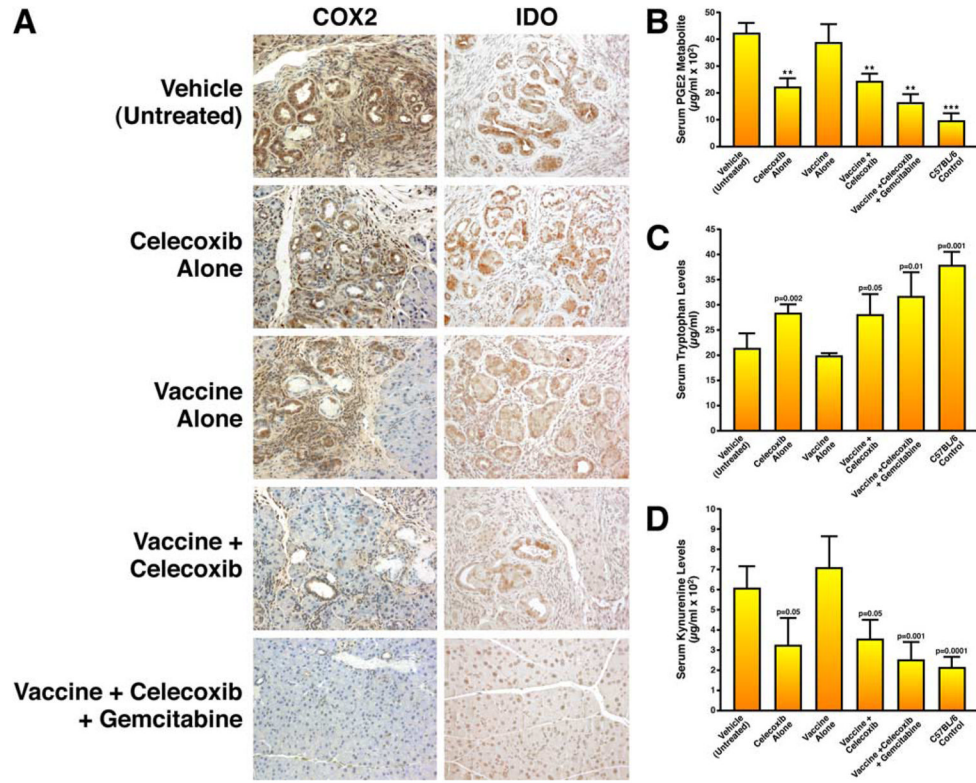
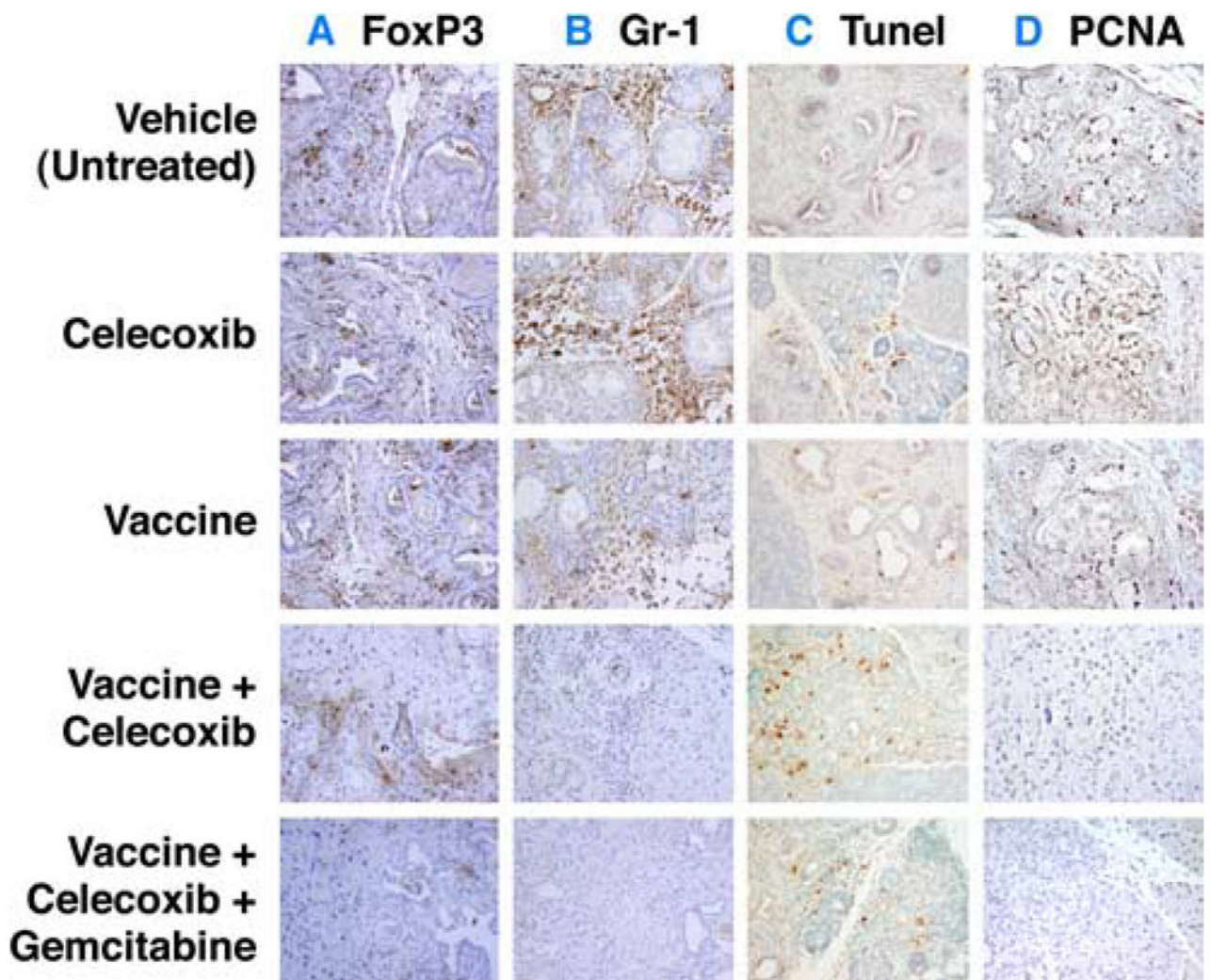


FIGURE 5. COX-2 and IDO expression and function is significantly reduced in PDA.MUC1 mice treated with the combination of vaccine plus celecoxib ± gemcitabine. *A*, Representative IHC images of COX-2 and IDO staining intensity of pancreas section from one mouse per treatment group; Brown staining represents COX-2 or IDO positivity. *n* = 6 mice per time point have been evaluated with similar results. Images were captured at ×200 magnification. *B*, Circulating levels of PGE₂ metabolite in PDA.MUC1 mice with various treatment regimens, **, *p* < 0.01; ***, *p* < 0.0001 compared with vehicle-treated mice; average of 15 mice are shown. *C* and *D*, Circulating levels of tryptophan (*C*) and kynurenine (*D*) in PDA.MUC1 mouse treated with various treatment regimens. Individual mouse data with *p* values are shown. Significance (*p* values) is calculated in comparison with the vehicle-treated mice. Nontumor-bearing C57BL/6 age-matched mouse sera were used as control.

**FIGURE 6.**

A and *B*, Decreased FoxP3⁺ and Gr-1⁺ infiltrating cells in pancreas tumor of PDA.MUC1 mice treated with the combination regimen. Representative IHC images of pancreas sections from mice treated with vehicle, celecoxib, vaccine, vaccine plus celecoxib, and vaccine plus celecoxib plus gemcitabine. *A*, FoxP3⁺ cells (representing Tregs) infiltrating the tumor bed. *B*, Gr-1⁺ cells (representing MSCs) infiltrating the tumor stromal areas surrounding the epithelial tumors. *n* = 15 mice were evaluated with similar results. *C* and *D*, Increased apoptotic (TUNEL⁺) cells and decreased proliferating (PCNA⁺) cells in situ in pancreas of PDA.MUC1 mice treated with the combination regimen. Representative IHC images of pancreas sections stained for TUNEL (*C*) or PCNA (*D*) to assess level of apoptosis or proliferation respectively. *n* = 15 mice have been assessed with similar results. Images were captured at ×200 magnification.